CICE2023 Rio de Janeiro - Brazil 11TH INTERNATIONAL CONFERENCE ON FRP COMPOSITES IN CIVIL ENGINEERING

BENDING AND SHEAR BEHAVIOR OF HISTORIC WALLS STRENGTHENED WITH COMPOSITE REINFORCED MORTAR

Tommaso D'Antino, Politecnico di Milano, Italy, tommaso.dantino@polimi.it
Veronica Bertolli, Politecnico di Milano, Italy, veronica.bertolli@polimi.it
Alessandro Cagnoni, Politecnico di Milano, Italy, alessandro.cagnoni@polimi.it
Angelo Savio Calabrese, Politecnico di Milano, Italy, angelosavio.calabrese@polimi.it
Carlo Poggi, Politecnico di Milano, Italy, carlo.poggi@polimi.it

ABSTRACT
Composite reinforced mortar (CRM) is a relatively new solution for the strengthening of existing masonry members that comprises fiber-reinforced polymer (FRP) grids reinforcing inorganic mortar overlays. CRMs were proven to be effective in strengthening masonry members against in- and out-of-plane loads. In this paper, a glass FRP-CRM is employed to strengthen 5-leaf historic masonry walls cut from an existing building located in Milan, Italy. The walls were strengthened and then subjected to three-point bending and diagonal compression tests. Results were compared with those of corresponding non-strengthened walls and showed the CRM effectiveness also in the case of thick masonry members.

KEYWORDS
Composite reinforced mortar; CRM; historic masonry; externally bonded reinforcement.

INTRODUCTION
Externally bonded (EB) composites are nowadays commonly employed in the strengthening of existing concrete (Brückner et al., 2006; Täljsten & Blanksvärd, 2007) and masonry (Papanicolaou et al., 2008) structures. Among them, fiber-reinforced polymers (FRP) have gained large popularity in the last few decades due to their high strength-to-weight ratio and ease of installation (Carloni & Subramaniam, 2009; Focacci & Carloni, 2015; Foraboschi, 2004). Recently, a new type of EB composites where the organic matrix was replaced with an inorganic mortar was proposed to overcome some of the drawbacks related to the use of epoxy resin, such as the FRP poor compatibility with the substrate and the lack of vapor permeability (Alecci et al., 2016). Different names were given to these composites depending on the type of inorganic binders and high-strength fibers employed. Among these, textile reinforced mortar (TRM) and fiber-reinforced cementitious matrix (FRCM) are commonly employed to identify composites comprising high-strength fiber textiles embedded within cement- or lime-based mortar matrices (D'Antino et al., 2014; D'Antino & Papanicolaou, 2017; Loreto et al., 2014).

In addition to inorganic-matrix EB composites, composite reinforced mortar (CRM) represents a relatively new strengthening solution for existing masonry structures. CRM comprises an FRP grid embedded within an inorganic mortar with an overall thickness of approximately 30 mm (Del Zoppo et al., 2019), which is three-four times that of FRCMs (D'Antino et al., 2019). The bi-directional FRP grid is made of laminated and pultruded yarns arranged in a mesh with clear spacing (i.e., edge-to-edge distance) usually equal to or higher than 30 mm (Del Zoppo et al., 2019). The cross-sectional area of each yarn is one order of magnitude higher than that of FRCMs (D'Antino et al., 2019). In CRM, fiber grids are usually made of glass fibers and are embedded in low strength mortar that is responsible for the good compatibility between the CRM and substrate. The application of CRM consists in fixing the grid to the support using metallic or FRP anchors and then plastering or even spraying the mortar. The grid is responsible for the reinforcement load-carrying capacity, while the mortar transfers the stress from the grid to the masonry substrate.

The rapidity of application and relatively low price of the grid and mortar make CRM systems a cost-effective strengthening solution. Furthermore, the use of an FRP grid, which does not suffer of corrosion, allows for retaining the CRM properties even in aggressive environments(D'Antino et al., 2023). CRM was proven to be effective in improving the in-plane (D'Antino et al., 2019; Prota et al., 2006) and out-of-plane (Donnini et al., 2021) displacement capacity of masonry walls, which is fundamental in case of seismic actions on the structure. Furthermore, the CRM reinforcement increases the masonry strength and creates a structural system with increased stiffness, deformation capacity, and energy dissipation (D'Antino et al., 2020). Acceptance criteria for CRM systems were published in Italy (CSLLPP - Servizio Tecnico Centrale, 2019) and in Europe (European Organisation for Technical Assessment (EOTA), 2018), but they are mainly focused on fiber grid and anchor mechanical properties rather than on the CRM system.

In general, the in-plane behavior of masonry walls is assessed by means of diagonal shear tests, which allow for obtaining useful information on the shear capacity of masonry walls avoiding complex procedures needed when both vertical (orthogonal to the bed joints) and horizontal (parallel to the bed joints) forces have to be applied at the same time to closely replicate the real conditions of the wall. During diagonal shear tests, a compressive load is applied along one of the two wall diagonals inducing tensile stresses in the orthogonal direction. Two different set-ups were adopted in the literature. In one case the wall is placed vertically (bed joints parallel to the ground) with the compressive force applied along one of its diagonals (Babaeidarabad et al., 2014; Carozzi et al., 2018; Menna et al., 2015), while in the other the wall is rotated so that one of its diagonal is parallel to the ground (i.e., with bed joints placed at an angle of 45° with respect to the ground), and the compressive force is applied along the vertical direction (Parisi et al., 2013). The out-of-plane behavior of masonry walls strengthened with EB inorganic-matrix composites is usually determined by three-point bending tests (Babaeidarabad et al., 2014; Donnini et al., 2021; Verderame et al., 2019). In general, the test is performed applying a horizontal force at mid height of the wall, orthogonal to the wall surface (Donnini et al., 2021). Sliding and overturning of the wall are hindered by two supports positioned at the bottom and top edges of the wall surface opposite to that where the load is applied. However, different test set-ups are proposed in the literature (see e.g., Babaeidarabad et al. (Babaeidarabad et al., 2014), where a distributed surface load was applied to one surface of the wall).

In this paper, the in-plane and out-of-plane behavior of CRM-strengthened 5-leaf historic masonry walls cut from an existing building were investigated by means of two in-plane diagonal compression tests and five out-of-plane three-point bending tests, respectively. The CRM studied comprised a glass fiber composite grid and a lime-based mortar and was applied on one or on both sides of the wall specimens. Results of tests performed on the strengthened walls were compared with those of corresponding non-strengthened (control) walls, showing the effectiveness of the CRM reinforcement in increasing both stiffness and strength of thick masonry walls.

MATERIALS AND METHODS

Material characterization

The 5-leaf historic masonry walls employed in this work were cut from a historic masonry building located in Milan, Italy. The masonry walls were made of irregular solid bricks and mortar joints with thickness ranging between 10 mm and 30 mm. The compressive properties of the walls were determined by uniaxial compression tests on two masonry blocks with dimensions 240×500×580 mm and 250×500×510 mm. Average values of compression strength, ultimate strain, and elastic modulus in compression obtained were 3.25-3.16 MPa, 0.45-0.67%, and 488-727 MPa, which resulted in average values of 3.21 MPa, 0.56%, and 607 MPa. The CRM employed to strengthen the existing walls comprised a bidirectional glass fiber open-mesh grid (TCS srl., 2020b) embedded in a 20 mm-thick hydraulic lime-based mortar (TCS srl., 2020a). The grid was made of ECR glass fiber yarns impregnated with epoxy thermoset resin that provided for the durability of the grid. The nominal cross-sectional area of the grid was 10 mm^2 and 9.6 mm^2 in warp and weft direction, respectively. The grid had a rectangular mesh with center-to-center spacing of 40 and 80 mm for the warp and weft yarns, respectively. The glass FRP grid had elastic modulus, tensile strength, and ultimate strain in

tension in the warp(weft) direction equal to 40(57) GPa, 525(670) MPa, and 1.15(1.12)%, as declared by the manufacturer (TCS srl., 2020b). The mortar nominal compression strength declared by the manufacturer was greater than 5 MPa (TCS srl., 2020a). The reinforcement was applied to the walls with GFRP anchors specifically developed for the CRM employed, as shown in Figure 1 (TCS srl., 2020a).

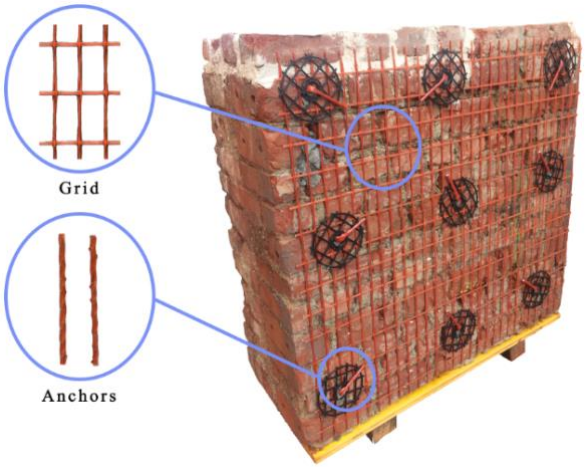

Figure 1: Application of the CRM grid to the specimen tested in diagonal compression

Three-point bending tests

To investigate the effectiveness of the CRM reinforcing system against out-of-plane loads, three-point bending tests were performed on two control (non-strengthened) and three strengthened masonry walls. Two out of three specimens were strengthened with one layer of CRM in tension and one layer in compression, while the remaining with a single layer in tension. The walls had length, *l*, 2000 mm and were characterized by a different cross-sectional area (*b*×*h*): 500×500 mm for the control specimens, 500×520 mm for the specimen with one layer of CRM, and 500×540 mm for the remaining specimens. The CRM layer was oriented to have warp yarns aligned with the longitudinal axis of the specimen, i.e., to maximize the grid cross-sectional area.

Tests were conducted using a three-point bending test set-up (Figure 2). The distance between the support axes, *L*, was equal to 1700 mm. The walls were laid on two supports (i.e., hinge on one side and roller on the opposite side) and a compression force was applied in the midspan cross-section using a servo-hydraulic jack equipped with a 300 kN loading cell. To better reproduce the real field conditions of masonry walls, an axial compression force equal to F_a=90 kN (Figure 2a) was applied to the specimen to simulate the axial force in the wall. The axial force was applied using two servo-hydraulic jacks and two C-shaped steel profiles positioned at the wall edges and connected by through steel rods (Figure 2). To avoid local failure, a layer of high resistance mortar was applied on the specimens at all loading and supports areas.

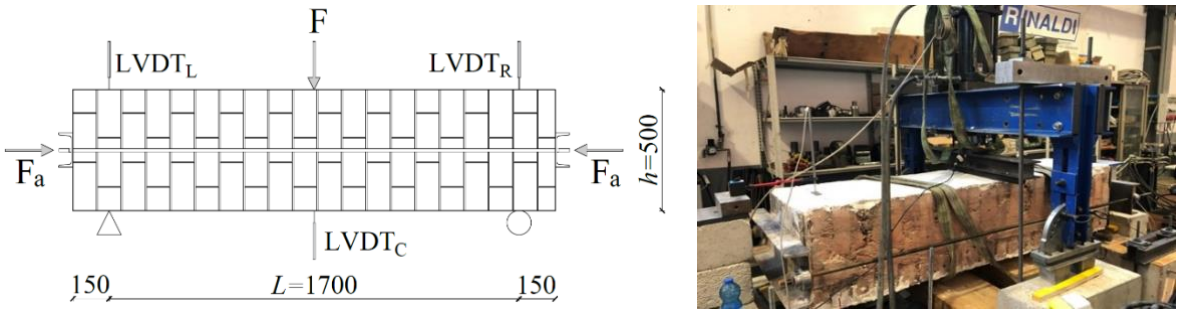

a) b)

Figure 2: a) Sketch of the three-point bending test set-up and b) specimen F_R_1 before testing (dimensions in mm)

Three LVDTs having gauge length of 100 mm were used to measure vertical displacements during the tests. One LVDT was placed at the wall midspan ($LVDT_C$) while the two remaining LVDTs were placed at the supports ($LVDT_L$ and $LVDT_R$). Tests were conducted in displacement control, increasing the stroke of the hydraulic jack at a constant rate of 0.005 mm/s.

Specimens were named following the notation F_X_N, where F=flexural, X=NR or R (NR=not reinforced and R=CRM-reinforced), and N=specimen number. Specimen F_R_3 was strengthened with a single layer of CRM, positioned on the tensile face.

Diagonal compression tests

To investigate the effectiveness of the CRM strengthening system against in-plane shear actions, diagonal compression tests were performed on two historic masonry walls. The first test was performed on the non-strengthened (control) masonry wall, having width *w* and height *h* equal to 1250 mm, and thickness *t* equal to 520 mm, while the second test was performed on the strengthened wall, which was CRM-reinforced on both sides and had dimensions 1200×1200×560 mm (*w*, *h*, and *t*).

Due to the large size of the historic walls tested, diagonal shear tests were performed with a horizontal test set-up (Figure 3). Indeed, the wall was placed horizontally, resting on four rollers (one at each corner), and the compressive load was applied in the horizontal direction along one of the two diagonals. The compression load was transferred to the specimen by means of two V-shaped steel profiles having 120 mm-long flanges. The load was applied by means of a servo-hydraulic jack equipped with a 1000 kN loading cell (Figure 3a) and connected to a rigid frame fixed to the laboratory strong floor. Before testing, a thin layer of mortar was applied to the top and bottom surfaces of the specimen so that all the measurement instruments could be accurately positioned. Furthermore, a layer of high strength mortar was applied to the wall edges in contact with the steel profiles to avoid possible local failures. With the same purpose, two neoprene sheets were placed between the wall and the steel profiles. Four LVDTs with gauge length of 100 mm were installed on the wall surfaces to measure the displacements along the diagonals. Two LVDTs were positioned on the top surface and two on the bottom surface of the wall, (see Figure 3b). They were positioned at approximately 280 mm from the corners along the wall diagonals and with a gauge length, l_0, variable between 826 mm and 869 mm. Tests were conducted increasing the stroke of the hydraulic jack at a constant rate of 0.030 mm/s.

Specimens were named following the notation CD_X_N, where CD=diagonal compression, X=NR or R (NR=not reinforced and R=CRM reinforced), and N=specimen number.

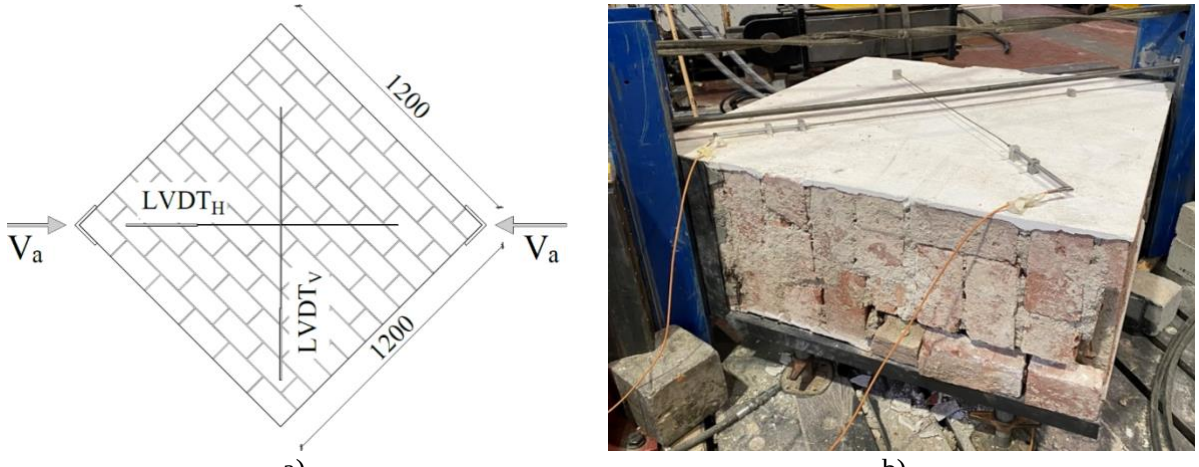

a) b)

Figure 3: a) Sketch of the diagonal compression test set-up and b) specimen CD_NR before testing (dimensions in mm)

RESULTS AND DISCUSSION

Three-point bending tests

For each specimen tested, the deflection at midspan, δ, was computed as the difference between the displacement recorded by $LVDT_C$, δ_C, and the average value of the recordings of $LVDT_L$ and $LVDT_R$, i.e., δ_L and δ_R:

$$\delta=\delta_C-(\delta_L+\delta_R)/2 \qquad \text{Eq. 1}$$

The applied force F - deflection δ and the bending moment M - deflection δ curves of the wall tested are reported in Figure 4a and Figure 4b, respectively, where $M=FL/4$ is the bending moment at midspan. The non-reinforced specimen F_NR_1 showed a linear branch interrupted by a brittle failure, whereas the nominally equal non-reinforced specimen F_NR_2 showed a non-linear branch before sudden failure. These specimens provided a similar peak load, although specimen F_NR_2 reached a higher ultimate deflection. This was attributed to differences in the two masonry specimens (e.g., mortar joint thickness, brick dimensions and layout), since they were cut from an existing historic building. Specimens reinforced with CRM showed an initial linear behavior followed by a non-linear branch before the attainment of a brittle failure. Specimen F_R_3 showed higher ultimate deflection and lower initial stiffness (i.e., slope of the linear branch) with respect to specimens F_R_1 and 2.

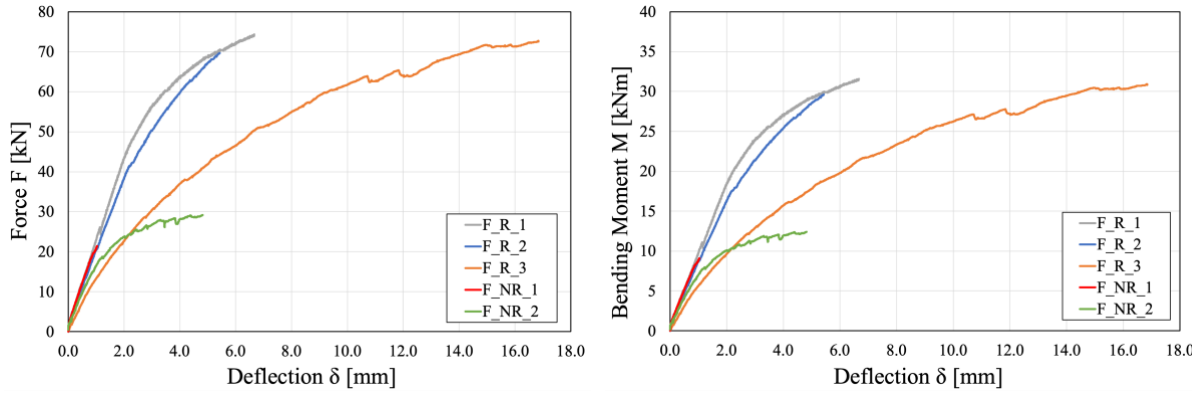

a) b)

Figure 4: Three-point bending tests: a) force - deflection and b) bending moment - deflection curves

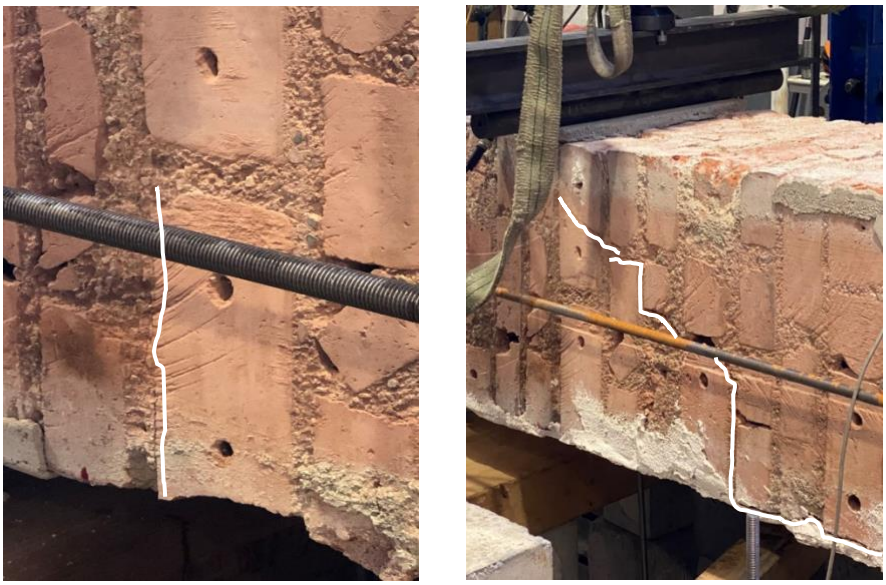

a) b)

Figure 5: a) Bending failure of specimen F_NR_1 and b) shear failure of specimen F_R_1

Control specimens attained failure due to the opening of a single flexural crack at midspan that developed between one brick and the adjacent mortar joint (Figure 5a). CRM-reinforced specimens reached failure due to the opening of a shear crack that crossed the bricks and the interfaces between bricks and mortar bed and head joints (Figure 5b). No detachment of the CRM was observed during the tests. The increase of peak load observed in strengthened specimens represents a lower bound since the failure mode shifted from bending to shear.

The peak load, F_{max}, the corresponding deflection (i.e., ultimate midspan deflection, δ_u) and bending moment, M_u, are reported in Table 1 for each specimen, along with their average values and coefficients of variation (CoV). Table 1 also reports the theoretical resisting bending moment M_{Rd} of the strengthened and control walls as well as the ratio between ultimate and resisting bending moments (M_u/M_{Rd}). The resisting bending moment was computed by cross-section equilibrium, considering the mechanical and geometrical parameters of the walls reported above. For specimens with CRM reinforcement, an average increase in peak strength of 89% with respect to the control specimen was observed. The specimen with one layer of CRM in tension (F_R_3) showed an ultimate load consistent with that of specimens F_R_1 and 2, confirming the negligible effect of the CRM in compression on the ultimate bending moment of the wall. The presence of the CRM reinforcement generally entailed for increasing the wall ultimate deflections. However, specimen F_R_1 and 2 reported δ_u in the range 5.43-6.67 mm, whereas specimen F_R_3 provided δ_u=16.85 mm. This difference was attributed to different wall geometrical and mechanical properties, as in the case of control specimens.

The experimental ultimate bending moment was lower than the theoretical resisting bending moment for all specimens (Table 1). Indeed, specimens failed in shear and could not fully develop their bending strength.

Table 1: Experimental results of three-point bending tests

Sample	F_{max} [kN]	$F_{max,avg}$ (CoV%) [kN]	δ_u [mm]	$\delta_{u,avg}$ (CoV%) [mm]	M_u [kNm]	$M_{u,avg}$ (CoV%) [kNm]	M_{Rd} [kNm]	M_u/M_{Rd} [-]
F_NR_1	47.24	38.25 (33%)	1.04	2.93 (91%)	9.11	10.75 (22%)	24.69	0.37
F_NR_2	29.25		4.82		12.40			0.50
F_R_1	74.35	72.25 (3%)	6.67	9.65 (65%)	31.60	30.67 (3%)	62.67	0.50
F_R_2	69.68		5.43		29.61			0.47
F_R_3	73.41		16.85		30.79		57.89	0.53

Diagonal compression tests

For each specimen tested, following the prescriptions of ASTM E519/E519M-22 (ASTM International, 2015), the shear stress τ was computed as:

$$\tau=0.707V/A_n \quad \text{Eq. 2}$$

Where V is the applied load and A_n is the net area of the specimen, i.e., the area of the wall cross-section considering only the solid part of the masonry units. Since solid bricks were employed, the net area A_n was taken equal to the total area of the specimen (i.e., $A_n=(w+h)t/2$).
The shear strain γ was computed as:

$$\gamma=|\varepsilon_c|+\varepsilon_t \quad \text{Eq. 3}$$

Where $\varepsilon_c=1/2\Sigma\Delta x_i/l_{0,i}$ and $\varepsilon_t=1/2\Sigma\Delta y_i/l_{0,i}$. Δx_i are the displacements measured along the diagonal in compression (i=1, 2 represents the displacement recorded on the top and bottom sides of the wall, respectively), and Δy_i are the displacements measured along the diagonal in tension (i=1, 2 represents

the displacement recorded on top and bottom sides of the wall, respectively). $l_{0,i}$ is the corresponding gauge length.

Experimental shear stress τ – shear strain γ curves are reported in Figure 6 and show consistency with the idealized τ - γ relationship reported in the literature (D'Antino et al., 2019). The strengthened specimen curve was characterized by an initial elastic branch followed by a pseudo-ductility branch during which the stresses in the wall are redistributed in the reinforcement grid. The control wall showed a brittle failure mode, characterized by the formation of a single crack along the diagonal in compression (Figure 7a). The CRM-reinforced wall showed several cracks during the first phase of loading, mostly concentrated at the corners where the steel profiles were located. Then, one main crack developed across the entire wall with an inclination angle lower than 45° with respect to the compressed diagonal direction (Figure 7b). At failure, portions of the reinforcing mortar layer detached from the wall (Figure 7c).

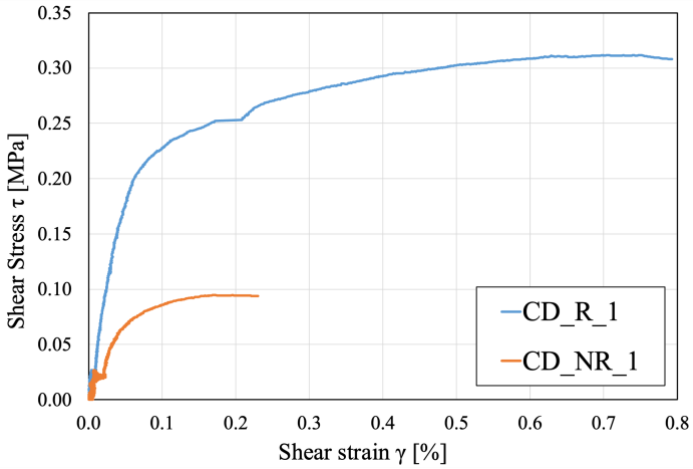

Figure 6: Shear stress τ – shear strain γ curves of the diagonal shear tests


a) b) c)

Figure 7: Failure mode of a) control, and CRM-reinforced wall b) during the initial part of the test and c) after failure

The peak load, V_{max}, corresponding shear stress, τ_{max}, and shear strain, γ_{max}, are reported in Table 2 for each specimen. Table 2 also reports the shear modulus, G, referred to as the modulus of rigidity by ASTM E519/E519M-22 (ASTM International, 2015), which was computed as the secant modulus between values equal to 20% and 50% of the peak shear stress (τ_{max}) on the experimental τ-γ curve:

$$G = \frac{\tau_{50} - \tau_{20}}{\gamma_{50} - \gamma_{20}} \quad \text{Eq. 4}$$

Table 2 - Experimental results of diagonal compression tests

Specimen	V_{max} [kN]	τ_{max} [MPa]	γ_{max} [mm/mm]	G [MPa]
CD_NR_1	87.12	0.095	0.00170	123
CD_R_1	296.23	0.312	0.00704	387

Results in Table 2 and Figure 6 show that the reinforcing system drastically increased the shear resistance of the masonry walls. Indeed, the strengthened specimen showed an increase in peak load of 240% with respect to the control specimen. In addition, the shear modulus G increased from 123 MPa to 387 MPa (increase of 314%). It should be noted that the value of maximum shear stress obtained for the control specimen is low if compared with experimental results reported in the literature (Donnini et al., 2021). Again, this could be attributed to irregularities in geometry and mechanical properties of walls tested, since they were cut from an existing building.

CONCLUSIONS

In this paper, the in-plane and out-of-plane behavior of glass CRM-strengthened 5-leaf historic masonry walls was investigated. Three CRM-reinforced specimens were subjected to three-point bending tests, while one was subjected to diagonal shear test. Due to the large size of the specimen, a specific test set-up was employed to investigate the in-plane shear behavior of the masonry wall. Results of the CRM strengthened specimens showed increase in peak strength, deformation capacity, and ultimate deflection (for the bending tests) when compared with the corresponding control specimens, which confirmed the effectiveness of the CRM reinforcement in the case of thick masonry members. However, the use of walls cut from an existing building entailed for a large scatter among the results.

ACKNOWLEDGEMENT

The experimental tests described in this paper were carried out at the Laboratorio Prove Materiali of the Politecnico di Milano, Italy. TCS s.r.l. is gratefully acknowledged for providing the composite materials.

CONFLICT OF INTEREST

The authors declare that they have no conflicts of interest associated with the work presented in this paper.

DATA AVAILABILITY

Data on which this paper is based is available from the authors upon reasonable request.

REFERENCES

Alecci, V., Focacci, F., Rovero, L., Stipo, G., & De Stefano, M. (2016). Extrados strengthening of brick masonry arches with PBO–FRCM composites: Experimental and analytical investigations. *Composite Structures*, *149*, 184–196. https://doi.org/10.1016/j.compstruct.2016.04.030

ASTM International. (2015). *Standard Test Method for Diagonal Tension (Shear) in Masonry Assemblages. ASTM E519/E519M*.

Babaeidarabad, S., Caso, F. D., & Nanni, A. (2014). Out-of-Plane Behavior of URM Walls Strengthened with Fabric-Reinforced Cementitious Matrix Composite. *Journal of Composites for Construction*, *18*(4), 04013057. https://doi.org/10.1061/(ASCE)CC.1943-5614.0000457

Brückner, A., Ortlepp, R., & Curbach, M. (2006). Textile reinforced concrete for strengthening in bending and shear. *Materials and Structures*, *39*(8), 741–748. https://doi.org/10.1617/s11527-005-9027-2

Carloni, C., & Subramaniam, K. V. (2009). Investigation of the interface fracture during debonding between FRP and masonry. *Advances in Structural Engineering*, *12*(5), 731–743. Scopus. https://doi.org/10.1260/136943309789867890

Carozzi, F. G., D'Antino, T., & Poggi, C. (2018). In-situ experimental tests on masonry panels strengthened with Textile Reinforced Mortar composites. *Procedia Structural Integrity*, *11*, 355–362. https://doi.org/10.1016/j.prostr.2018.11.046

CSLLPP - Servizio Tecnico Centrale. (2019). *Linea Guida per la identificazione, la qualificazione ed il controllo di accettazione dei sistemi a rete preformata in materiali compositi fibrorinforzati a matrice polimerica da utilizzarsi per il consolidamento strutturale di costruzioni esistenti con la tecnica dell'intonaco armato CRM (Composite Reinforced Mortar)*.

D'Antino, T., Bertolli, V., Pisani, M. A., & Poggi, C. (2023). Tensile and interlaminar shear behavior of thermoset and thermoplastic GFRP bars exposed to alkaline environment. *Journal of Building Engineering*, *72*, 106581. https://doi.org/10.1016/j.jobe.2023.106581

D'Antino, T., Calabrese, A. S., & Poggi, C. (2020). Experimental procedures for the mechanical characterization of composite reinforced mortar (CRM) systems for retrofitting of masonry structures. *Materials and Structures*, *53*(4), 94. https://doi.org/10.1617/s11527-020-01529-1

D'Antino, T., Carloni, C., Sneed, L. H., & Pellegrino, C. (2014). Matrix–fiber bond behavior in PBO FRCM composites: A fracture mechanics approach. *Engineering Fracture Mechanics*, *117*, 94–111. https://doi.org/10.1016/j.engfracmech.2014.01.011

D'Antino, T., Carozzi, F. G., & Poggi, C. (2019). Diagonal shear behavior of historic walls strengthened with composite reinforced mortar (CRM). *Materials and Structures*, *52*(6), 114. https://doi.org/10.1617/s11527-019-1414-1

D'Antino, T., & Papanicolaou, C. (2017). Mechanical characterization of textile reinforced inorganic-matrix composites. *Composites Part B: Engineering*, *127*, 78–91. https://doi.org/10.1016/j.compositesb.2017.02.034

Del Zoppo, M., Di Ludovico, M., Balsamo, A., & Prota, A. (2019). In-plane shear capacity of tuff masonry walls with traditional and innovative Composite Reinforced Mortars (CRM). *Construction and Building Materials*, *210*, 289–300. https://doi.org/10.1016/j.conbuildmat.2019.03.133

Donnini, J., Maracchini, G., Lenci, S., Corinaldesi, V., & Quagliarini, E. (2021). TRM reinforced tuff and fired clay brick masonry: Experimental and analytical investigation on their in-plane and out-of-plane behavior. *Construction and Building Materials*, *272*, 121643. https://doi.org/10.1016/j.conbuildmat.2020.121643

European Organisation for Technical Assessment (EOTA). (2018). *CRM (Composite Reinforced Mortar) Systems for Strengthening Concrete and Masonry Structures. EAD 340392-00-0104*. EOTA.

Focacci, F., & Carloni, C. (2015). Periodic variation of the transferable load at the FRP-masonry interface. *Composite Structures*, *129*, 90–100. Scopus. https://doi.org/10.1016/j.compstruct.2015.03.008

Foraboschi, P. (2004). Strengthening of masonry arches with fiber-reinforced polymer strips. *Journal of Composites for Construction*, *8*(3), 191–202. Scopus. https://doi.org/10.1061/(ASCE)1090-0268(2004)8:3(191)

Loreto, G., Leardini, L., Arboleda, D., & Nanni, A. (2014). Performance of RC slab-type elements strengthened with fabric-reinforced cementitious-matrix composites. *Journal of Composites for Construction*, *18*(3). Scopus. https://doi.org/10.1061/(ASCE)CC.1943-5614.0000415

Menna, C., Asprone, D., Durante, M., Zinno, A., Balsamo, A., & Prota, A. (2015). Structural behaviour of masonry panels strengthened with an innovative hemp fibre composite grid. *Construction and Building Materials*, *100*, 111–121. https://doi.org/10.1016/j.conbuildmat.2015.09.051

Papanicolaou, C. G., Triantafillou, T. C., Papathanasiou, M., & Karlos, K. (2008). Textile reinforced mortar (TRM) versus FRP as strengthening material of URM walls: Out-of-plane cyclic loading. *Materials and Structures/Materiaux et Constructions*, *41*(1), 143–157. Scopus. https://doi.org/10.1617/s11527-007-9226-0

Parisi, F., Iovinella, I., Balsamo, A., Augenti, N., & Prota, A. (2013). In-plane behaviour of tuff masonry strengthened with inorganic matrix–grid composites. *Composites Part B: Engineering*, *45*(1), 1657–1666. https://doi.org/10.1016/j.compositesb.2012.09.068

Prota, A., Marcari, G., Fabbrocino, G., Manfredi, G., & Aldea, C. (2006). Experimental in-plane behavior of tuff masonry strengthened with cementitious matrix-grid composites. *Journal of Composites for Construction*, *10*(3), 223–233. Scopus. https://doi.org/10.1061/(ASCE)1090-0268(2006)10:3(223)

Täljsten, B., & Blanksvärd, T. (2007). Mineral-based bonding of carbon FRP to strengthen concrete structures. *Journal of Composites for Construction*, *11*(2), 120–128. Scopus. https://doi.org/10.1061/(ASCE)1090-0268(2007)11:2(120)

TCS srl. (2020a). *Technical datasheet of B-STRUCTURA G*. (Italy). https://www.tcscalce.it/categoria/consolidamento

TCS srl. (2020b). *Technical datasheet of TCS glass MR48*. (Italy). https://www.tcscalce.it/categoria/consolidamento

Verderame, G. M., Balsamo, A., Ricci, P., Di Domenico, M., & Maddaloni, G. (2019). Experimental assessment of the out-of-plane response of strengthened one-way spanning masonry infill walls. *Composite Structures*, *230*, 111503. https://doi.org/10.1016/j.compstruct.2019.111503